Green Chemistry

PAPER

View Article Online
View Journal | View Issue

Published on 30 September 2021. Downloaded by UNIVERSITY OF CINCINNATI on 8/23/2022 3:27:18 AM.

Check for updates

Cite this: *Green Chem.*, 2021, **23**, 8501

Milligram-scale, temperature-controlled ball milling to provide an informed basis for scale-up to reactive extrusion†

Joel Andersen, *[a] Hunter Starbuck, [a,b] Tia Current, [a,b] Scott Martin[c] and James Mack [b]

Received 18th June 2021,
Accepted 30th September 2021

DOI: 10.1039/d1gc02174e

rsc.li/greenchem

Over the last several years, chemists and engineers have identified the utility of using twin-screw extruders for performing large-scale organic chemistry mechanochemically. This equipment is convenient as it is familiar to several relevant industries for its use in formulation, and it is also well-equipped for temperature control and intense grinding of materials. However, the research and development scale of mechanochemistry is just like that of conventional synthesis: milligrams. These milligram-scale reactions are performed in batch-type reactors, often a ball mill. Commercially available ball mills do not have strict temperature control, limiting the information that can be obtained to inform the scale-up process reliably. This work uses an in-house modified, temperature-controlled, ball mill to bridge the knowledge gap regarding predictable, well-informed, economical, and reliable mechanochemical scale-ups. Included in this work is the first extrusion example of a nucleophilic aromatic substitution.

Introduction

Mechanochemistry—replacing solvents with mechanical forces to facilitate mixing—has made significant strides in becoming a more commonplace tool in the toolbox of chemistry. Several reviews[1–3] have highlighted its utility towards organic[4–7] and inorganic[8,9] synthesis alike. Part of the impetus behind this progress comes from two rapidly developing areas of mechanochemistry: (1) *in situ* reaction monitoring by analytical methodologies such as PXRD,[10,11] Raman,[12,13] solid-state NMR,[14] and simultaneous combinations thereof[15–18] and (2) temperature-controlled milling.[19–27] These two aspects are vital to the adoption of any new chemical methodology. They help provide some of the necessary insights sought by chemists or engineers interested in a third critical aspect: scale-up. Mechanochemical scale-up has thus far been performed *via* single-screw,[28] or, more commonly, twin-screw extrusion[29–36] (Fig. 1). Twin-screw extrusion is a continuous process in which materials are fed into rotating screws that simultaneously grind and convey a material down a temperature-controlled barrel. However, without specific knowledge regarding the reaction robustness at a variety of temperatures at the small scale, it is difficult to get 'buy-in' from a process or manufacturing chemist. This is especially true when a reaction involves high-value, low-volume chemicals such as an active pharmaceutical ingredient intermediate. Thus, although industry has expressed growing interest in this exciting chemistry, reservations remain.

Part of these reservations can be addressed by accelerating the interplay between the three areas (*in situ* monitoring, temperature control, and scale-up). These areas have developed so rapidly and recently that connections between them have been limited. Prior work from a collaboration of Stuart James' group and Duncan Browne's group previously explored the process of translating milling results to an extrusion process.[33] Their work especially highlights the translation of LAG from milling to extrusion. The present work seeks to build upon that paper by begin bridging the gap between two of the areas mentioned above: temperature-controlled reaction development in milligram-scale, ball-mill reactions and large-scale synthesis *via* twin-screw extrusion. The missing component is that temperature-control is a standard feature of twin-screw extruders, but it is not currently a feature in commercially available ball mills. In this work, we pair our in-house modified, temperature-controlled ball mill with a twin-screw extruder to investigate the correlation between the temperature-control capabilities of the two reactors.

One limitation of extruder equipment is their brief residence times.[29–31,36] The residence time is a distribution describing the amount of time most particles spend in a reac-

[a]*Cinthesis, 301 Clifton Court, Cincinnati, OH 45221, USA.*
E-mail: Joel.Andersen@CinthesisSolutions.com
[b]*University of Cincinnati, 301 Clifton Court, Cincinnati, OH 45221, USA*
[c]*ThermoFisher Scientific, 2 Radcliff Road, Tewksbury, MA 01876, USA*

†Electronic supplementary information (ESI) available. See DOI: 10.1039/d1gc02174e

Published on 30 September 2021. Downloaded by UNIVERSITY OF CINCINNATI on 8/23/2022 3:27:18 AM.

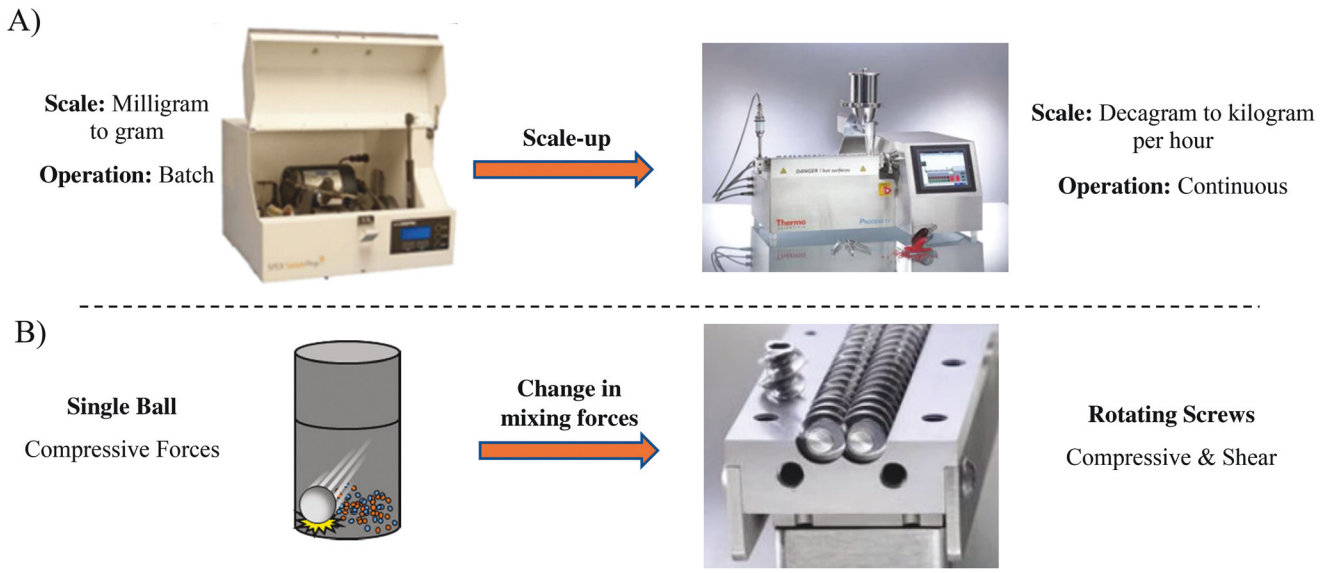

Fig. 1 (A) Aspects of ball milling and extrusion. (B) Comparison of the forces that facilitate mixing. Mixing in a ball mill with a single ball is dominated by compressive forces, but extruders have a significant additional component of shearing. The reader is cautioned that mechanochemical literature now largely indicates that although mechanical forces maintain mixing, it is the bulk temperature that provides the energy for overcoming activation barriers.

tive zone—in this case, the extruder's barrel. Unlike solvent-based, continuous-flow reactors, the reactive zone cannot be made arbitrarily long. Conventional extrusion processes may have a residence time between one and three minutes.[37] However, residence times in the range of five to fifteen minutes are (thus far) achievable.[38] This means a reaction must be complete within that time—a challenging requisite for many reactions. Fortunately, this pairs well with the ubiquitous rate enhancements associated with performing reactions in the absence of solvent.[25] This time constraint sets the stage for the first step of testing a reaction for scale-up to extrusion: ball mill reactions should last just five to fifteen minutes. This mandate forces considerations regarding the time required to heat the small-scale reaction vessel and the way in which the proportional-integral-derivative (PID) temperature controller heats the system, and it is where we began our investigation.

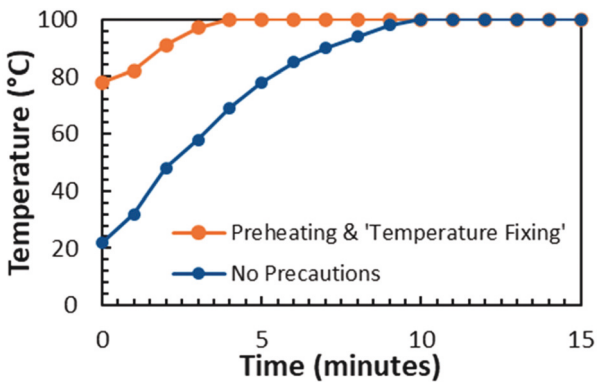

Fig. 2 Heating rates of a mechanochemical reactor to be used for a short reaction time (15 minutes or less).

Results and discussion

In our initial experience, PID-controlled heating of a ball-mill reaction took ten minutes to warm from room temperature to the target temperature of 100 °C (>8 minutes to be within 5 °C), as seen in Fig. 2. To minimize heating times, two precautions were taken: (1) equipment was pre-heated prior to being charged with reactants (**CAUTION:** the experimenter should have a good understanding of a reaction's exothermicity well before this, see SI) and (2) the PID controller's target temperature was set above the desired reaction temperature by 10 °C and adjusted to the target temperature upon the PID's measured temperature getting within one or two degrees of the target temperature. The first precaution is simply a direct time save by putting the bulk of the heating prior to any possible reaction. The second is based on PID mathematics. PID controller designs/settings often operate in a manner to minimize unintended 'overshooting' at the cost of approaching the target in an asymptotic-like fashion. Although selected somewhat arbitrarily, the 10 °C adjustment was effective in our experience and would suggest the same adjustment for other setups where the temperature increase is too slow for the length of an experiment. An experienced user can alter PID controller settings by modifying tuning constants used in the mathematics: K_p (proportional gain), K_i (integral gain), and K_d (derivative gain). We elected for the simpler approach of providing a higher target and then adjusting the set target manually. The revised heating profile can be seen in Fig. 2. This figure indicates that for reactions lasting five to fifteen

 This journal is © The Royal Society of Chemistry 2021

Published on 30 September 2021. Downloaded by UNIVERSITY OF CINCINNATI on 8/23/2022 3:27:18 AM.

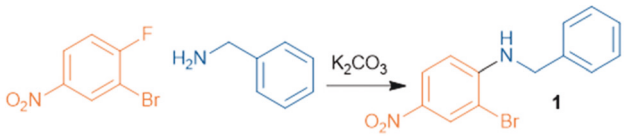

Fig. 3 Nucleophilic aromatic substitution reaction.

minutes, the two precautions can lead to more meaningful control of temperature.

With a reactor that had more accurate heating, we began our investigation by targeting the nucleophilic aromatic substitution reaction (S_NAr) shown in Fig. 3. A 2016 review of medicinal chemistry papers found that S_NAr reactions are indispensable.[39] Unfortunately, they are preferably performed in polar, aprotic solvents such as dimethylformamide (DMF) due to mechanistic considerations. Environmental considerations and potential legislation in Europe restricting these solvents encouraged our reaction choice.[40,41]

We started with the S_NAr reaction in Fig. 3 as our model reaction. The conversion to product was measured over time at 40 °C and is presented in Fig. 4. Since we need to achieve complete conversion in 15 minutes, we then performed the reaction at a variety of temperatures in our ball mill for 15 minutes, as seen in Fig. 5. The mixture appears to proceed through a point at about ~85–90% conversion where increasing the temperature seems to have limited effect. We attribute this to mixing challenges as opposed to energetics. One must keep in mind that, in contrast to a homogeneous solution, a solvent-free reaction mixture's physicochemical properties are constantly evolving. As a reaction proceeds, the distribution of starting materials, intermediates, and products changes. Arguing from the standpoint of the Arrhenius Equation, when molecules at higher temperatures do not achieve higher conversions, we must presume that they are not colliding as frequently, all other things being equal. Thus, we conclude that the mobility of molecules at this point in the reaction may be the inhibiting factor. Nonetheless, we do see that we can eventually achieve full conversion at 110 °C. Interestingly, we determined the melting point of the purified product be 107.6–108.0 °C. Although mechanochemical reactions do not require reactants to melt, it is possible that the phase change in this case is especially helpful by allowing easier mixing.[42] In any event, this informs us that sides reactions do not appear at increasing temperatures in the relevant range and that we can expect to identify similar conditions in the extruder that will provide us with full conversion if we can achieve a residence time similar to the fifteen minute reaction time used in the mill.

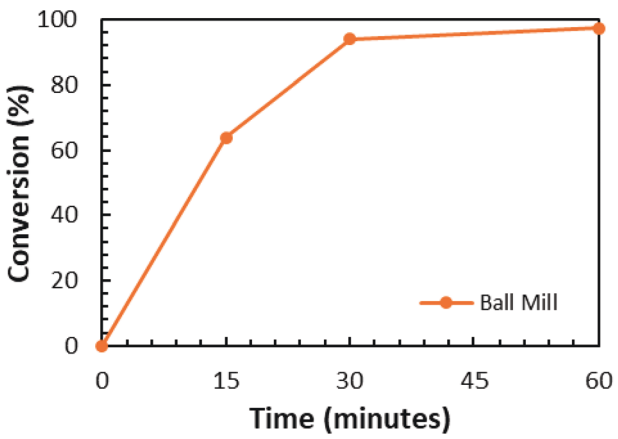

Fig. 4 S_NAr reaction conversion over time in the ball mill at 40 °C.

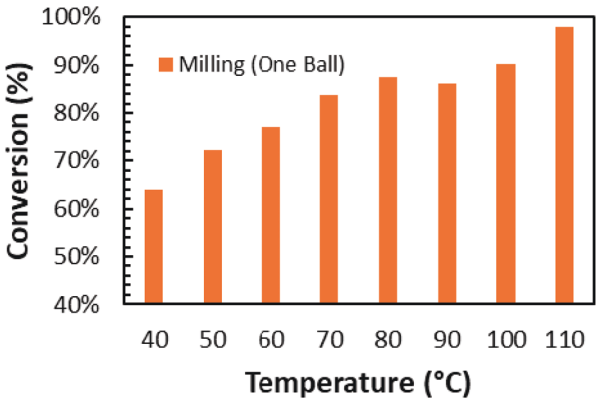

Fig. 5 Conversion at a variety of temperatures in the mill. The reaction was stopped after fifteen minutes in all cases.

We can now begin considering the extrusion side of things. Screw design and its relationship with residence time reactive extrusion is a rapidly evolving area of interest. Historically, extruders are designed with short (<5 minutes) residence times. With the advent of reactive extrusion, however, long residence times would be highly desirable. The individual elements making up a screw can have a variety of characteristics. These elements may efficiently propel material down the barrel with very limited mixing ("conveying" elements) or do so in a slower manner with more mixing and an increased residence time ("forwarding" elements). Alternating 90° elements maximizes mixing without any forwarding characteristics at the cost of building up increased back pressure and torque. Finally, reversing elements can add extra resistance to flow, causing intense mixing and higher pressures (and torques). Long residence times must be balanced with the maximum torque an extruder can achieve, as well as corresponding heat build-up. For more information, please see the ESI.† To achieve a long residence time, prior experience in the extrusion field led to the screw design seen in Fig. 6. With this screw configuration in place, we began testing the reaction in the extruder using extrusion parameters portrayed in Fig. 7.

We started by determining the residence time at our lowest temperature (40 °C). It is a mistake to assume the residence time is the elapsed time between turning on the feeders and the first appearance of material at the barrel outlet. During that time, the extruder is not operating at steady state. Instead, we used pulse experiments to determine the residence time. In

Published on 30 September 2021. Downloaded by UNIVERSITY OF CINCINNATI on 8/23/2022 3:27:18 AM.

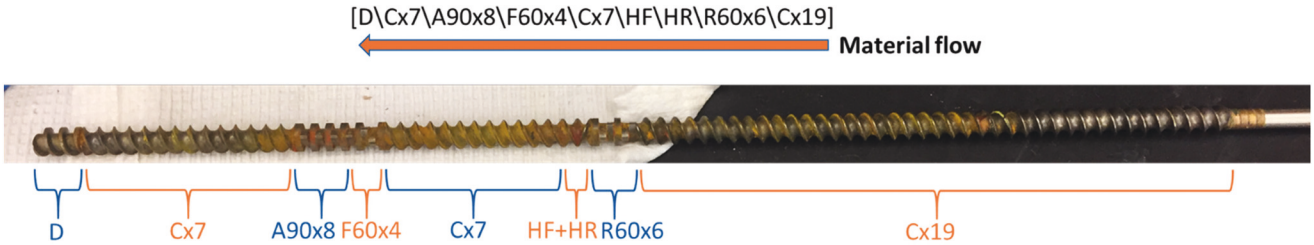

Fig. 6 Screw configuration tested for the S_NAr reaction between benzylamine and 3-bromo-4-fluoro-nitrobenzene. Naming convention: [letter (s)][angle] × [number]. The letter describes the type (or arrangement) of element(s): D = discharge; C = conveying; A = alternating; R = reversing, F = forwarding, H = half. The angle describes the offset (in degrees) from prior element. The number describes the number of $\frac{1}{4}$ L : D elements (or $\frac{1}{2}$ when half is used). More information on screw design is available in the ESI.†

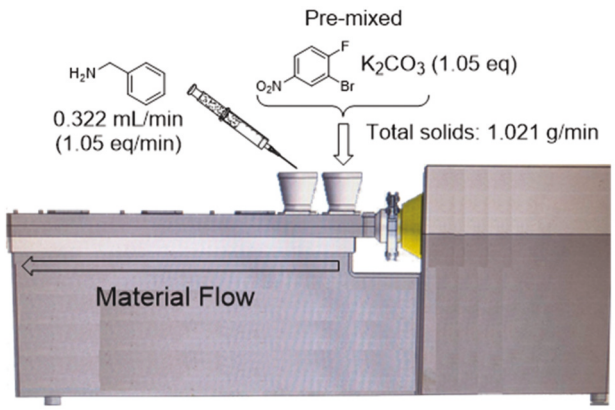

Fig. 7 Extrusion parameters for the S_NAr reaction. The arrow indicates the direction of flow of material down the extruder barrel.

a pulse experiment, a single spike of a tracer chemical (food coloring) is delivered directly to the inlet port on the extruder and a timer is started. The output of the barrel can then be monitored for the appearance of the tracer. As expected from a system producing a distribution of residence times, the tracer does not exit the barrel as the same "spike" that it entered as. Instead, the intensity of the tracer varies over time as it exits the barrel as a dispersion rather than as a spike. For best determination of the residence time range, video was recorded and reviewed later. Prior to determining the residence time, it is suggested to monitor the torque to ensure it has leveled off, which is a good indicator of reaching steady-state conditions (see SI for further details on residence time determination). With the screw design described above and parameters as described in Fig. 7, our residence time range was approximately 10–16 minutes. Thus, a significant portion of molecules will proceed through the reactor faster than the 15-minute milling reaction time and a small portion will proceed more slowly. For our purposes, the match was close enough to continue and obtain conversion data at the different temperatures explored in the mill.

When taking samples for conversion analysis, we elected to wait one residence time after changing temperatures, as well as one residence time between samples. For that purpose, we approximated the residence time to be 15 minutes. Results of this approach are provided in Fig. 8. This figure presents several interesting findings to consider. Firstly, the initial extrudate (defining time zero) was analyzed, although it should not be considered meaningful since the extruder is not operating at steady-state conditions. In comparison, conversions at time points 15, 30, and 45 minutes are in good agreement, and all are within rounding error of 47%. Pleasingly, stepwise increases in temperature led to stepwise increases in conversion. Just as we observed in the temperature-controlled mill, the reaction inevitably marched toward quantitative conversion (in the extruder, 98%, 97%, and 98% were the three samples taken at the final temperature). A one-minute sample (1.323 g) was collected and underwent liquid–liquid extraction and column chromatography. This sample indicated an isolated yield of 97% (details in SI). To facilitate comparison with milling, the three data points taken at each temperature were averaged and plotted in a bar-chart format in Fig. 9. In this figure there are three striking observations readily made.

First, the triads of data points are consistent within each temperature, indicative of a steady-state process. Second, although the extruder initially provides lower conversions than the mill, it ultimately leads to higher conversions at higher temperatures. Third, the extruder does not exhibit the inhibition observed in the mill at higher conversions (there was no

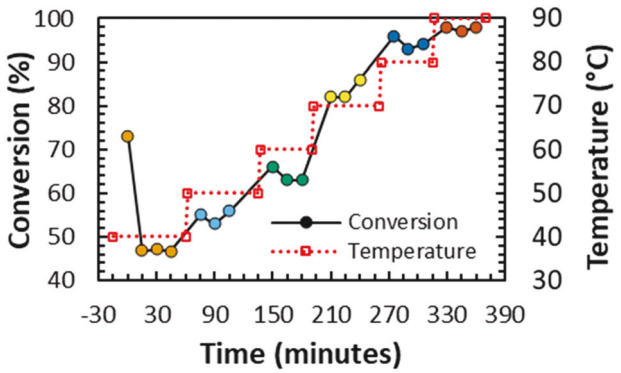

Fig. 8 Extrusion results for the model S_NAr reaction. Data points that share color are taken at the same temperature.

This journal is © The Royal Society of Chemistry 2021

Published on 30 September 2021. Downloaded by UNIVERSITY OF CINCINNATI on 8/23/2022 3:27:18 AM.

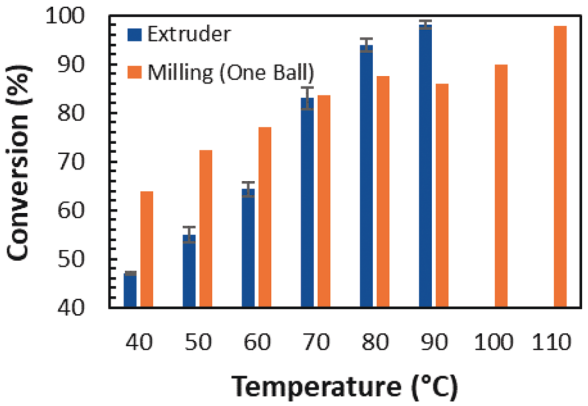

Fig. 9 Comparison of extrusion results and ball mill (with one ball) results at matching temperatures. The reader is encouraged to recall that the residence time (extruder) and reaction time (mill) do not perfectly match.

need to go beyond 90 °C). The second observation can be readily explained by considering two different effects that are taking place. At lower conversions, mixing is not notably inhibited in the mill, and the reaction time in the mill is longer than the effective reaction time most molecules experience in the extruder. At higher conversions, the reaction time continues to be longer in the mill, but the mixing of the mill is not sufficient to maintain a well-mixed environment. This limits molecular collisions by inefficiently clearing product "out of the way", thus limiting reaction rate as has been explored by Stuart James.[43] This supposition would necessitate that the mixing in the extruder outperforms that of the mill. This is reasonable as there are significant shear forces in the extruder whereas the mill is limited to compressive forces when a single ball is used, as was the case in our ball milling experiments. To attempt to improve mixing while limiting frictional heating, we introduced an additional ball and obtained the results in Fig. 10, which are in good agreement with the

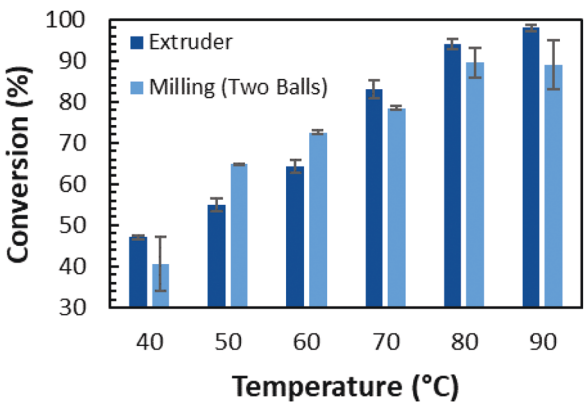

Fig. 10 Comparison of extrusion results and ball mill (with two balls) results at matching temperatures. The reader is encouraged to recall that the residence time (extruder) and reaction time (mill) do not perfectly match.

extruder and appear to have somewhat alleviated the mixing issue. With these explanations of the two observations, the results are straight-forward and provide powerful testimony to the usefulness of small-scale research and development work using temperature-controlled ball-mill reactors for enabling an informed scale-up process.

With respect to the work-up and its corresponding environmental impact, this reaction can be purified in a couple ways depending on the needed product purity. If 97% purity is sufficient, then a water wash of the product will remove salt byproducts. If higher purity is needed, recrystallization is a likely route. Regardless of the chosen route, the removal of water-miscible polar, aprotic reaction solvents simplifies and improves the work-up as they are often challenging to remove *via* distillation and are often diluted into large volumes of water which must then be disposed of in accordance with environmental regulations.[44] Solvent selection guides strongly discourage the use of these solvents when possible.[45]

Knoevenagel reaction

Following the success of the S_NAr reaction, we elected to investigate the Knoevenagel reaction between vanillin and barbituric acid (outlined in Fig. 11). This reaction has been intensively studied in small-scale mechanochemical reactors,[18,21,46–50] and it was also part of the landmark paper describing reactive twin-screw extrusion for chemical synthesis purposes.[31] Despite this, some details of the reaction remain intriguing. For example, James *et al.* observed sigmoidal kinetics when performing the reaction mechanochemically, as reproduced here in Fig. 12(A).[48] Several reasons for this were explored, but after experimentally excluding their possibilities, the authors found experimental evidence indicating that the reaction mixture progresses and reaches a point whereat it becomes hard enough to generate heat build-up from the striking ball. They found this consistent with the observed temperature progressions noted in Fig. 12(B). Interestingly, when the same authors performed the reaction in an extruder (without the additional 10% water), they found that, despite initial appearances of product at 40 °C, full conversion was not achieved until 160 °C (the melting points of vanillin and barbituric acid are 83 °C and 245 °C, respectively).

Two follow-up studies by Užarević *et al.*[24] and Halasz *et al.*,[50] both performed in ball mills, discovered the formation of a co-crystal that forms rapidly when milling the two starting materials. Although the co-crystal does have an orientation

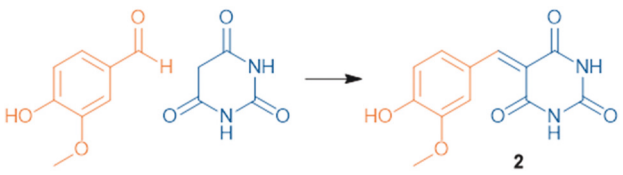

Fig. 11 Knoevenagel reaction between vanillin and barbituric acid.

Published on 30 September 2021. Downloaded by UNIVERSITY OF CINCINNATI on 8/23/2022 3:27:18 AM.

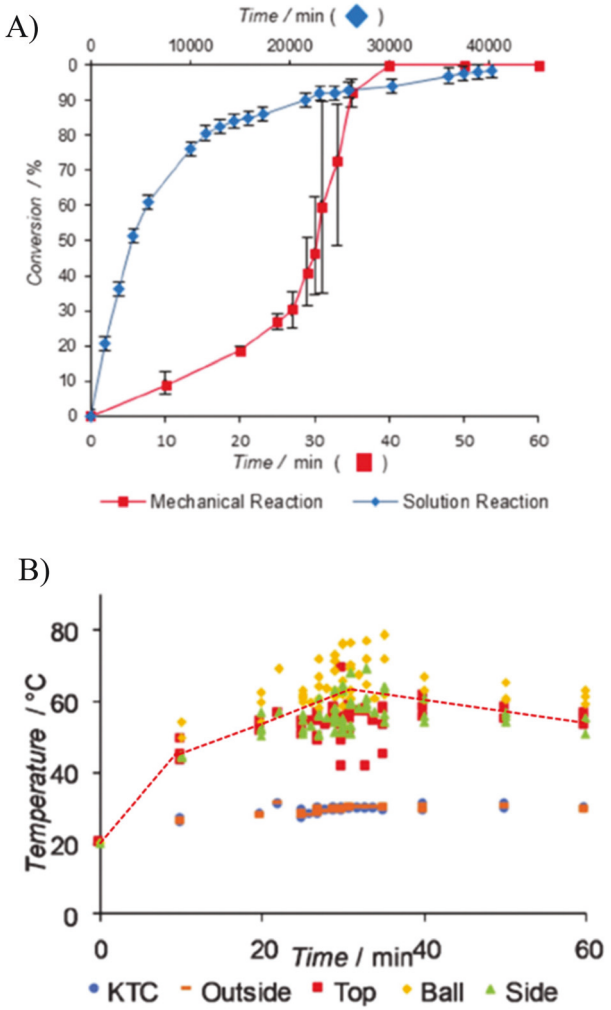

Fig. 12 (A) Sigmoidal kinetics observed for the mechanochemical Knoevenagel reaction in comparison to the conventional solution behavior. (B) Temperatures observed during the experiment. The dashed red line is not in the original figure and is our estimate of an "effective" representative temperature. Reproduced with permission from ref. 48.

that could allow for reactivity, it is not necessarily the most energetically favorable orientation. They found that by incorporating small amounts of an appropriate liquid (0–2 μL liquid per mg reaction mixture)—known as liquid-assisted grinding (LAG)—co-crystallization could be circumvented, resulting in reaction rate enhancements. Thus, it may be the case that this co-crystal restricts the mobility of the reagents to achieve the lowest energy conformation for reactivity. Although they explored several liquids, they did not describe results where water was the LAG agent as was the case in the work by James *et al.* (0.5 μL liquid per mg reaction mixture).

Given the number of variables regarding mixing and temperature control, we thought that this reaction would be interesting to use as a second model reaction for scale-up. Presumably, by understanding better what is happening on a small-scale, we will be better equipped to scale-up in a timely and economical manner when using reactants that are more valuable.

Since the first objective was to better understand and control the reaction better on the small scale, we estimated the "effective" temperature of the system from James' work over time. We have represented this with a dashed red line, superimposed over the authors' original data, in Fig. 12(B). We then manually adjusted a PID controller in a ball-mill reactor to determine how well we would reproduce the prior work's estimated temperature profile. We also obtained the profile of our system when heated to a constant 60 °C using the same heating precautions applied earlier. These temperature profiles are presented in Fig. 13(A). The constant temperature of 60 °C was chosen as it is roughly the estimated temperature at the steepest part of the sigmoidal curve. By employing both profiles, we were able to test (1) if we could reproduce the sigmoidal kinetics and (2) if we could obtain a kinetic curve more consistent with the conventional curve in Fig. 12(A). Indeed, as shown in Fig. 13(B), the results of running these reactions with the prescribed temperature profiles showed success in both objectives. Further discussion on sigmoidal curves and milling without temperature control is provided in the SI. We additionally performed the reaction for a fixed time (five

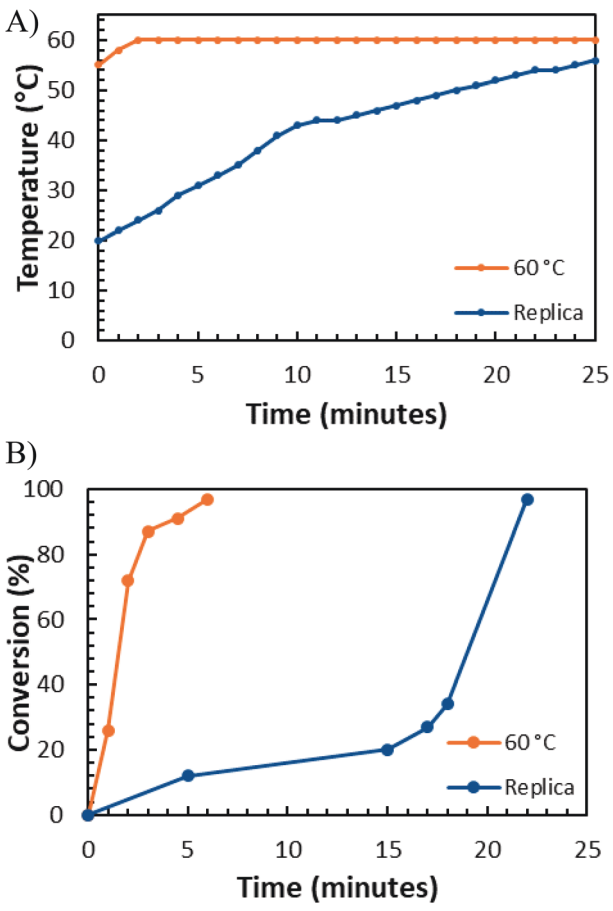

Fig. 13 Kinetic data for the Knoevenagel reaction. (A) Measured temperatures from temperature-controlled reactions at a constant 60 °C and under our replica system. (B) Reaction conversion when performed under the two temperature profiles from A.

This journal is © The Royal Society of Chemistry 2021

Published on 30 September 2021. Downloaded by UNIVERSITY OF CINCINNATI on 8/23/2022 3:27:18 AM.

minutes) at a variety of temperatures leading up to the previously tested 60 °C. The results of these tests can be seen in Fig. 14. Interestingly, this reaction rate seems far more temperature sensitive than the previously explored S_NAr reaction. Armed with an improved understanding, we felt comfortable and confident in proceeding to the larger-scale extruder work.

Initial attempts to run the Knoevenagel reaction were performed with the same screw configuration used for the S_NAr reaction. However, we observed excessive heat build-up occurring in the barrel, especially in the mixing zones, when using the same screw configuration that we used for the S_NAr reaction. In our experience, this reaction can produce very hard, tough-to-break-up mixtures. Thus, although we were pleased with the residence time (nine to 15 minutes), we elected to modify the screw design. An ideal screw design will provide the longest possible residence time while minimizing any heat build-up or torque overages (exceeding the maximum torque for which the equipment is designed). Since the materials in this case are cheap, we elected to explore a variety of screw designs with the idea in mind to develop a library of screw designs for different mixing challenges. Working through a variety of screw designs is a time-, material-, and labor-intensive process, so the development of such libraries would prove very helpful. Future studies that allow the use ball-mill results to predict an appropriate screw design from the library would further expedite this process. The results of the various screw designs are provided in Table 1. Drawing broad conclusions from these data is challenging. However, it is clear that the torque is strongly related to temperature rises for the physical properties of these materials. Based on the results of Table 1, we elected to proceed with Screw Configuration 3 using the parameters from Entry 1 of Table 2 as it provided the best balance of residence time and heat build-up and an opportunity to look at how the comparison holds when the reaction time is even shorter than the 15 minutes allowed for the S_NAr reaction.

The results of performing the Knoevenagel reaction in the extruder are provided in Fig. 15, and the milling results have been included for ease of comparison. Just as with the S_NAr reaction, we found the data encouraging. Given that the residence time (extruder) and reaction time (mill) is not (and, essentially, cannot be) a perfect match, there can always be some difference expected between milling and extrusion, but the good agreement between methodologies show that there is great utility in combining temperature-controlled milling and

Table 2 Feeder and Barrel parameters for knoevenagel extrusion

Entry	Barrel RPMs	Feeder (g min^{-1})	Water feed rate (mL min^{-1})	Residence time (min)
1	50	1.2	0.12	4 : 30–7 : 00
2	50	0.6	0.06	6 : 00–10 : 00
3	25	0.6	0.06	3 : 00–8 : 00

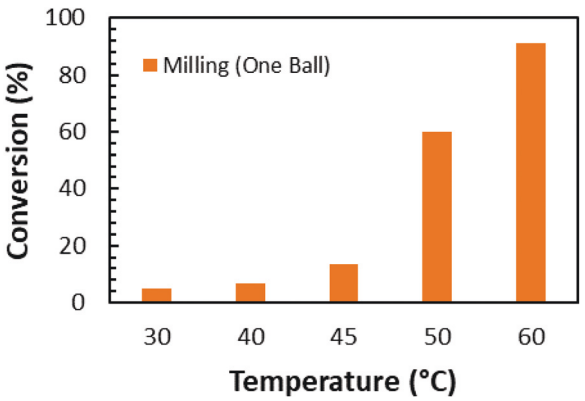

Fig. 14 Effect of temperature on the milligram-scale ball-milled Knoevenagel reaction.

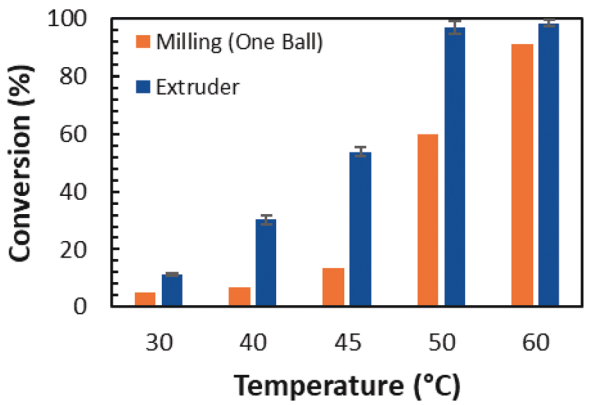

Fig. 15 Comparison of ball milling and extruder results for the Knoevenagel reaction.

Table 1 Residence time and heat build-up resulting from using a variety of screw configurations

Configuration ID	Mixing section 1	Mixing section 2	Mixing section 3	Residence time (min)	Temperature (target = 35 °C)	Torque (% of maximum)
1	A90 × 8\F60 × 4	HF\HR\R60 × 6	Conveying	9 : 00–15 : 00	49	48
2	R60 × 4	HF\HR\R60 × 4	Conveying	4 : 15–8 : 05	45	35
3	R60 × 4	F30 × 4\R60 × 4	Conveying	4 : 30–7 : 15	36–37	12
4	R60 × 4	F30 × 4\R60 × 4	F30 × 7\R60 × 3	3 : 00–5 : 41	40	35
5	R60 × 4	HF\HR\R60 × 4	F30 × 10	2 : 30–5 : 15	44	37
6	R60 × 4	R60 × 3\A90 × 5	F30 × 10	3 : 00–6 : 30	42	34

Naming convention is identical to Fig. 5. Further discussion is presented in the ESI.†

Published on 30 September 2021. Downloaded by UNIVERSITY OF CINCINNATI on 8/23/2022 3:27:18 AM.

reactive extrusion as a powerful duo. Of note from the data is that full conversion can be achieved at significantly lower temperatures in comparison to performing the extrusion without 10% added water (160 °C without *vs.* 50 °C to 60 °C with). Given the 1 : 1 stoichiometry and the success of the reaction, the only work-up needed is drying to remove the water byproduct of the reaction. In previous literature this was done naturally as the barrel was already at 160 °C, thus forcing the water to leave as steam. In our case, elevating the temperature at the end of the barrel will affect the conversion. Instead, a sample of extrudate (1.211 g) was worked-up, resulting in an isolated yield of 95% for the 60 °C reaction in the extruder (see SI), which is consistent with the conversion indicated in the figure.

When we attempted the extrusion without added water, we experienced a torque overage (using Screw Configuration ID 1). Notably, vanillin is insoluble in water, but barbituric acid is soluble in water.[51] Thus, the addition of 10% (w/w) water (0.05 μL mg^{-1} reaction mixture, 0.80 equivalents) may minimize the formation of the co-crystal as was observed in the studies discussed earlier, allowing easier mixing and removing a barrier to molecular collisions. As discussed earlier, this is known as liquid-assisted grinding (LAG), and it is a common mechanochemical approach to altering product selectivity and/or enhancing reaction kinetic rates. A LAG experiment can be characterized by its η value, which is defined as the microliters of liquid divided by the total reaction mass. LAG occurs in the range $0 < \eta < 2.0$. When η exceeds 2.0, the system is more aptly described as a slurry. Identifying proper liquids for use in these systems is routine and easily achieved on the milligram scale. In addition to work by Browne *et al.*, these results provide further indication that a highly effective LAG additive (water, η = 0.05 μL mg^{-1}) identified on the small scale was also essential to successful scale-up.[33]

Conclusions

Reaction reliability and predictability are two essential characteristics required for smooth scale-up in industry. Using S_NAr and Knoevenagel model reactions, we have provided strong evidence in favor of using temperature-controlled milling for small-scale (milligram) research and development in preparation for scale-up *via* twin-screw extrusion. Temperature control on the small scale enables a more thorough understanding of the reaction with respect to rates and expectations that can be made for extrusion temperatures. We also propose the development of screw design libraries and look forward to the eventual development of a method for selecting a screw design based on ball-mill results (or other small-scale work).

Conflicts of interest

There are no conflicts to declare.

Author contributions

JA oversaw, planned, and performed the research and led manuscript creation. HS and TC assisted with performing the experiments and data collection. SM provided insights regarding screw configuration design. JM assisted with data interpretation and experimental design. All authors assisted with manuscript support.

Acknowledgements

JA would like to acknowledge funding from the University of Cincinnati's 1819 Innovation Hub. HS, TC, and JM would like to acknowledge funding from the National Science Foundation (CHE-1900097).

References

1 J. L. Do and T. Friscic, *ACS Cent. Sci.*, 2017, **3**, 13–19.
2 T. Friscic, C. Mottillo and H. M. Titi, *Angew. Chem., Int. Ed.*, 2020, **59**, 1018–1029.
3 J. L. Howard, Q. Cao and D. L. Browne, *Chem. Sci.*, 2018, **9**, 3080–3094.
4 J. Andersen and J. Mack, *Green Chem.*, 2018, **20**, 1435–1443.
5 A. Stolle, T. Szuppa, S. E. Leonhardt and B. Ondruschka, *Chem. Soc. Rev.*, 2011, **40**, 2317–2329.
6 J. G. Hernandez and C. Bolm, *J. Org. Chem.*, 2017, **82**, 4007–4019.
7 D. Tan and T. Friščić, *Eur. J. Org. Chem.*, 2018, 18–33.
8 D. Tan and F. Garcia, *Chem. Soc. Rev.*, 2019, **48**, 2274–2292.
9 T. Stolar and K. Užarević, *CrystEngComm*, 2020, **22**, 4511–4525.
10 T. Friscic, I. Halasz, P. J. Beldon, A. M. Belenguer, F. Adams, S. A. Kimber, V. Honkimaki and R. E. Dinnebier, *Nat. Chem.*, 2013, **5**, 66–73.
11 T. Stolar, L. Batzdorf, S. Lukin, D. Zilic, C. Motillo, T. Friscic, F. Emmerling, I. Halasz and K. Uzarevic, *Inorg. Chem.*, 2017, **56**, 6599–6608.
12 D. Gracin, V. Strukil, T. Friscic, I. Halasz and K. Uzarevic, *Angew. Chem., Int. Ed.*, 2014, **53**, 6193–6197.
13 V. Strukil, D. Gracin, O. V. Magdysyuk, R. E. Dinnebier and T. Friscic, *Angew. Chem., Int. Ed.*, 2015, **54**, 8440–8443.
14 J. G. Schiffmann, F. Emmerling, I. C. B. Martins and L. Van Wullen, *Solid State Nucl. Magn. Reson.*, 2020, **109**, 101687.
15 K. Uzarevic, I. Halasz and T. Friscic, *J. Phys. Chem. Lett.*, 2015, **6**, 4129–4140.
16 P. A. Julien, L. S. Germann, H. M. Titi, M. Etter, R. E. Dinnebier, L. Sharma, J. Baltrusaitis and T. Friščić, *Chem. Sci.*, 2020, **11**, 2350–2355.
17 L. Batzdorf, F. Fischer, M. Wilke, K. J. Wenzel and F. Emmerling, *Angew. Chem., Int. Ed.*, 2015, **54**, 1799–1802.
18 S. Haferkamp, F. Fischer, W. Kraus and F. Emmerling, *Beilstein J. Org. Chem.*, 2017, **13**, 2010–2014.

 This journal is © The Royal Society of Chemistry 2021

Published on 30 September 2021. Downloaded by UNIVERSITY OF CINCINNATI on 8/23/2022 3:27:18 AM.

19 M. F. Rene Eckert and F. Schüth, *Angew. Chem., Int. Ed.*, 2017, 2445–2448.
20 G. Kaupp, *CrystEngComm*, 2011, **13**, 3108–3121.
21 R. Schmidt, C. F. Burmeister, M. Baláž, A. Kwade and A. Stolle, *Org. Process Res. Dev.*, 2015, **19**, 427–436.
22 F. Fischer, K. J. Wenzel, K. Rademann and F. Emmerling, *Phys. Chem. Chem. Phys.*, 2016, **18**, 23320–23325.
23 J. Andersen and J. Mack, *Angew. Chem., Int. Ed.*, 2018, **57**, 13062–13065.
24 N. Cindro, M. Tireli, B. Karadeniz, T. Mrla and K. Užarević, *ACS Sustainable Chem. Eng.*, 2019, **7**, 16301–16309.
25 J. M. Andersen and H. F. Starbuck, *J. Org. Chem.*, 2021, DOI: 10.1021/acs.joc.0c02996.
26 J. M. Andersen and J. Mack, *Chem. Sci.*, 2017, **8**, 5447–5453.
27 J. Andersen, J. Brunemann and J. Mack, *React. Chem. Eng.*, 2019, **4**, 1229–1236.
28 B. M. Sharma, R. S. Atapalkar and A. A. Kulkarni, *Green Chem.*, 2019, **21**, 5639–5646.
29 D. Crawford, J. Casaban, R. Haydon, N. Giri, T. McNally and S. L. James, *Chem. Sci.*, 2015, **6**, 1645–1649.
30 D. E. Crawford, C. K. Miskimmin, J. Cahir and S. L. James, *ChemComm*, 2017, **53**, 13067–13070.
31 D. E. Crawford, C. K. G. Miskimmin, A. B. Albadarin, G. Walker and S. L. James, *Green Chem.*, 2017, **19**, 1507–1518.
32 K. J. Ardila-Fierro, D. E. Crawford, A. Körner, S. L. James, C. Bolm and J. G. Hernández, *Green Chem.*, 2018, **20**, 1262–1269.
33 Q. Cao, J. L. Howard, D. E. Crawford, S. L. James and D. L. Browne, *Green Chem.*, 2018, **20**, 4443–4447.
34 R. B. Carvalho and S. V. Joshi, *Green Chem.*, 2019, **21**, 1921–1924.
35 M. Ali El-Remaily, A. M. M. Soliman and O. M. Elhady, *ACS Omega*, 2020, **5**, 6194–6198.
36 D. E. Crawford, A. Porcheddu, A. S. McCalmont, F. Delogu, S. L. James and E. Colacino, *ACS Sustainable Chem. Eng.*, 2020, **8**, 12230–12238.
37 K. Paulsen, D. Leister and A. Gryczke, *Investigating process parameter mechanism for successful scale-up of a hot-melt extrusion process*, Application Notes LR-71, BASF SE, Lampertheim, Germany, 2013, https://tools.thermofisher.com/content/sfs/brochures/LR71-e-Investigating-Process-Parameter-Mechanism.pdf.
38 G. R. Ziegler and C. A. Aguilar, *J. Food Eng.*, 2003, **59**, 161–167.
39 D. G. Brown and J. Bostrom, *J. Med. Chem.*, 2016, **59**, 4443–4458.
40 L. Bergkamp and N. Herbatschek, *Rev. Eur. Comp. Int. Environ. Law*, 2014, **23**, 221–245.
41 M. C. Bryan, P. J. Dunn, D. Entwistle, F. Gallou, S. G. Koenig, J. D. Hayler, M. R. Hickey, S. Hughes, M. E. Kopach, G. Moine, P. Richardson, F. Roschangar, A. Steven and F. J. Weiberth, *Green Chem.*, 2018, **20**, 5082–5103.
42 T. Seo, K. Kubota and H. Ito, *J. Am. Chem. Soc.*, 2020, **142**, 9884–9889.
43 X. Ma, W. Yuan, S. E. Bell and S. L. James, *ChemComm*, 2014, **50**, 1585–1587.
44 A. C. Laurent Delhaye, P. Jacobs, C. Kottgen and A. Merschaert, *Org. Process Res. Dev.*, 2007, **11**, 160–164.
45 C. M. Alder, J. D. Hayler, R. K. Henderson, A. M. Redman, L. Shukla, L. E. Shuster and H. F. Sneddon, *Green Chem.*, 2016, **18**, 3879–3890.
46 G. Kaupp, M. Reza Naimi-Jamal and J. Schmeyers, *Tetrahedron*, 2003, **59**, 3753–3760.
47 R. Trotzki, M. M. Hoffmann and B. Ondruschka, *Green Chem.*, 2008, **10**, 873–878.
48 B. P. Hutchings, D. E. Crawford, L. Gao, P. Hu and S. L. James, *Angew. Chem., Int. Ed.*, 2017, **56**, 15252–15256.
49 S. Haferkamp, W. Kraus and F. Emmerling, *J. Mater. Sci.*, 2018, **53**, 13713–13718.
50 S. Lukin, M. Tireli, I. Loncaric, D. Barisic, P. Sket, D. Vrsaljko, M. di Michiel, J. Plavec, K. Užarević and I. Halasz, *ChemComm*, 2018, **54**, 13216–13219.
51 *CRC Handbook of Chemistry and Physics*, ed. R. C. Weast, CRC Press, Inc., Boca Raton, FL, 1982.